Effect of Graphene Nanosheets Reinforcement on the Mechanical Properties of Rubber Seed Oil Based Polyurethane Nanocomposites

E. O. Obazee and F. E. Okieimen

Abstract Graphene-reinforced polyurethane nanocomposites were prepared by catalytic reaction of dispersion of exfoliated graphene nanosheet/rubber seed oil polyol (Gr–RSOP) hybrid and polyisocyanates (hexamethylene diisocyanate, HMDI, and 4,4'-methylene-bis(phenylisocyanate, MDI), at equimolar reactant ratios (NCO/OH ratio of 1.0), to give samples Gr–PUH and Gr–PUM, respectively. The structure and morphology of the obtained nanocomposites were analyzed using X-ray diffraction, atomic force microscopy (AFM) and FT–IR, respectively, while the mechanical and thermal properties were determined using nanoindenter, universal testing machine and thermogravimetric analyzer. The X-ray pattern revealed exfoliated graphene nanosheets in the nanocomposites, while the structures of the neat polyurethanes and nanocomposites showed great similarity. The hardness, tensile strength, young modulus, and thermal stability showed varied improvement and a corresponding reduction in elongation attributed to graphene incorporation.

Keywords Graphene · Rubber seed oil · Polyol · Polyurethane · Nanocomposites · Property

Introduction

The high crystalline nature of graphite hinders large polymer molecules from filling the inter-layer space of its unit graphene sheets, thus making it unsuitable in polymer reinforcement, and hence the need for its modification to graphene. This can run from expanding graphite (by several oxidizing agents) [1, 2] to its exfoliation. Notable exfoliation techniques are micromechanical exfoliation, liquid-phase exfoliation, epitaxial growth on SiC and chemical vapor deposition (CVD) growth

E. O. Obazee (✉)
Rubber Research Institute of Nigeria, P. M. B 1049 Benin City, Nigeria
e-mail: efosaosagie@yahoo.cco.uk

F. E. Okieimen
Department of Chemistry and Center for Biomaterials Research, University of Benin, Benin City, Nigeria

T. S. Srivatsan and M. Gupta (eds.), *Nanocomposites VI: Nanoscience and Nanotechnology in Advanced Composites*, The Minerals, Metals & Materials Series, https://doi.org/10.1007/978-3-030-35790-0_12

[3–9]. Graphene is a two-dimensional or single-layer graphite packed in a honeycomb lattice [9–13] with a thickness of one single atom [14], which is thought to be the stiffest [3, 15] and strongest material in the world [16]. Intrinsic graphene is a semi-metal or zero-based gap semi-conductor [9] with unique properties that vary significantly from the bulk graphite and have greatly influenced its incorporation in new technologies [17]. Pristine graphene has amazing mechanical, electrical, chemical and thermal properties (high thermal conductivity approx. 5000 $Wm^{-1}K^{-1}$), an ultra-high intrinsic carrier mobility (~200, 000 $cm^2V^{-1}S^{-1}$), large theoretical surface area (~2630 $m^2\ g^{-1}$), and high theoretical transmittance (97.7%). All these qualities of pristine graphene make it promise in many applications [9], such as in transparent conductive films, transistors, super capacitors, sensors, and catalyst support [14, 18–23].

A major encumbrance in the use of pristine graphene material is the difficulty in obtaining the unmodified form and insolubility in all organic solvents, as the modified graphene does not retain the structural quality and exceptional properties (e.g., as electron mobility) found in the single-layer graphene [18, 24]. Graphite oxidation to graphene oxide (GO), via modified Hummers method, and the reduction of the obtained GO to reduced graphene oxide (rGO) is the commonest method used to produce graphene, but with distorted structure that cannot be fully restored [24, 25]. Also, rGO is susceptible to aggregation and requires surfactant or strong capping agent to improve dispersion due to its hydrophobicity, and thereby introduces impurity and thus disrupts the electrical structure of pristine graphene as the surfactant is difficult to remove [26–29].

Without significant modification, exfoliation of graphene from graphite in the liquid phase can be achieved using both aqueous and non-aqueous systems, in reasonable quantities for research purpose that can be scaled up. Unlike the non-aqueous system, the aqueous system of liquid-phase exfoliation of graphene is cheap, safer and environmentally friendly from the use of water, only requiring the addition of surfactant in order to get the best interfacial tension range for efficient exfoliation. Matching the cohesive energy of liquid phase to the cohesive energy of graphite promotes the separation of graphitic and graphene sheets under shear [30]. Liu et al. [15] and co-worker demonstrated that graphite flakes can be exfoliated to give graphene sheets that are well dispersed in ethanol/water mixture and stable for years without addition of any surfactants.

Though there are several nanoparticles that are currently used in the synthesis of polymer nanocomposites (PCN), such as clays, carbon nanotubes, silica nanoparticles, nanofibers, etc., graphene is outstanding. Graphene sheets can be used in hydrophobic and hydrophilic polymers and can furnish most of the possible merit of nanorange sized fillers [31–33]. The low cost, natural availability, combined with its good mechanical, thermal, and barrier properties makes graphene a choice nanoparticle for use in polymer nanocomposites that can offer possibilities for new material

development. Various methods that can be employed for the preparation of polymer graphene nanocomposites include solution blending [31, 34], exfoliation–adsorption [35], in situ intercalative polymerization [36] and melt intercalation [37].

There are some reports on expanded graphite or exfoliated GO, rGO, functionalized rGO, and nanocomposites based on a range of polymers [38–41] but there appear to be few reports on pristine graphene–polyurethane nanocomposites, and to the best of our knowledge, no report on rubber seed oil polyol based polyurethane nanocomposite. In this study, we report the preparation of rubber seed oil polyol (RSOP) based graphene-reinforced polyurethane nanocomposites.

Experimental

Materials and Methods

Mechanically expressed rubber seed oil (RSO) was obtained from Rubber Research Institute of Nigeria and used as received in the preparation of rubber seed oil polyol [42], physico-chemical properties given in Table 1. Laboratory grade graphite powder, −20–80 mesh, 99.9% (metal basis), was obtained from Alfa Aesar, USA. Hexamethylene diisocyanates (HMDI), 4,4'-methylene-bis(phenylisocyanate) (MDI), toluene, ethanol, dichloromethane, and dibutyltindilaurate (DBTDL) were obtained from Sigma Aldrich, India.

Table 1 Physico-chemical properties of RSOP

Properties	RSOP
Color	Orange-yellow
Density	1.019
AV ($mgKOHg^{-1}$)	14.733
SV ($mgKOHg^{-1}$)	239.17
IV ($gI_2 100\ g^{-1}$)	9.240
HV ($mgKOHg^{-1}$)	203.47
Oxirane content (%)	0.402
Mn ($g\ mol^{-1}$)	1014.68
Functionality	3.7524

Characterization Techniques

Structural and Morphological Analyses

Structural studies of the Polyurethane and nanocomposites samples were recorded using Agilent Technologies Cary 660 FTIR spectroscopy attached with attenuated total reflectance (ATR). Rigaku Smart lab Wide Angle X-ray Diffraction (WAXD) machine using CuKa radiation (at $\lambda = 1.54068$ A°) and a Bragg–Brentano geometry, equipped with X-ray generator set at 45kV tension and 100 mA current, a point proportional detector, and a curve quartz monochromator, a goniometer radius circle of 250 mm were used for examining the crystalline and morphology of the samples. A scanning rate of 0.02^{o}/s over range of 2θ (2–50^{o}) for one-dimensional X-ray diffraction (XRD) pattern on oriental samples suspended on a glass slide was used for the X-ray studies. Also, the Bruker Dimension ICON ScanAsyst Atomic Force Microscopy (AFM) was used for the surface morphology, using the tapping mode.

Physico-Mechanical Properties of Polyurethanes and Nanocomposites

Tinius Olsen H50KS Universal Testing Machine (using ASTM 6287-09 method, 50KN force at a speed of 50 mm/min and gauge length of 12.04) and Hystron TI 950 Triboindenter, with a standard diamond indenter probe, using ASTM E2546-07, were used for determining the tensile properties and hardness, respectively. The thermal stability of the samples was carried out with the Netzsch STA 449 FI Jupiter analyzer at a heating rate of 10 °C/min, to a temperature of 600 °C, using sample weight between 10 and 14 mg at 10 k/min in nitrogen. The degree of swelling of the polymers was carried out by immersing cut-and-weighed size pieces into a solution of toluene and taking the weight at interval at ambient temperature until a constant weight was obtained. At this point, the sample was blotted dry with a dry cloth and weighed. Duplicate experiment was carried out for each sample and the average was taken as the final weight [43].

Preparation of Graphene-Reinforced Polyurethane Nanocomposites

Exfoliation of Graphene Nanosheets

The method of Liu et al. [15]was used in the preparation of the mono- or few layered graphene (Gr), by sonication of graphite powder in ethanol/water solution. In a typical experiment, 1 g of graphite powder, −20–80 mesh and 99.9% metal basis, was weighed into a vial, and 40 ml solution of 70/30 ethanol/water solution was poured in. The mixture was shaken for about a minute and placed in an ultrasonic

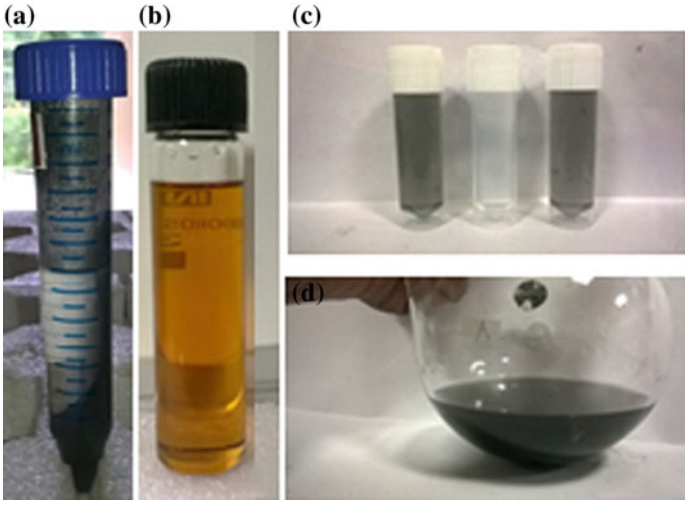

Fig. 1 **a** Centrifuged and sonicated graphite/graphene dispersion in ethanol–water. **b** RSOP. **c** Pipetted upper layer supernatant graphene dispersion (middle vial is ethanol–water reference). **d** Mixture of pipette graphene layer in ethanol–water and RSOP

water bath, at 25 °C, and dispersed for about 3 h, after which it was centrifuged for 60 min at 500 rpm. The supernatant upper layer graphene was pipetted off, using a micro-pipette, into a pre-weighed reactor flask, see Fig. 1a, c.

Preparation of Graphene–Rubber Seed Oil Polyol (RSOP) Hybrid

A calculated amount of rubber seed oil polyol (RSOP) (required in preparing polyurethanes at NCO/OH ratio 1.0) was added to the flask containing the as-obtained graphene dispersed in ethanol/water described above. The flask was swirled to dissolve the RSOP and to ensure proper mixing and placed in a rotary evaporator to remove the ethanol/water solution, first at 40 °C, and then at 80 °C, in a total of about 24 h, until the graphene–rubber seed oil polyol (Gr-RSOP) hybrid so obtained was solvent and moisture free.

Preparation of Polyurethanes and Graphene-Reinforced Polyurethane Nanocomposites

Into two quick-fit flasks containing Gr-RSOP hybrid obtained above and RSOP, respectively, under reflux and fitted with nitrogen gas inlet and was charged the required amount of DBTDL catalyst and toluene, and stirred to enable proper mixing in an inert atmosphere. Then the calculated amount of HMDI required to give an NCO/OH ratio of 1.0 was calculated (see recipe on Table 2), and was charged into the

Table 2 Recipe of graphene-reinforced polyurethanes nanocomposites

Samples	Ingredients	Graphene content (%)
PUH	RSOP—HMDI (NCO/OH ratio 1.0)	0
Gr–PUH	RSOP—HMDI (NCO/OH ratio 1.0)	0.13
PUM	RSOP—MDI (NCO/OH ratio 1.0)	0
Gr–PUM	RSOP—MDI (NCO/OH ratio 1.0)	0.13

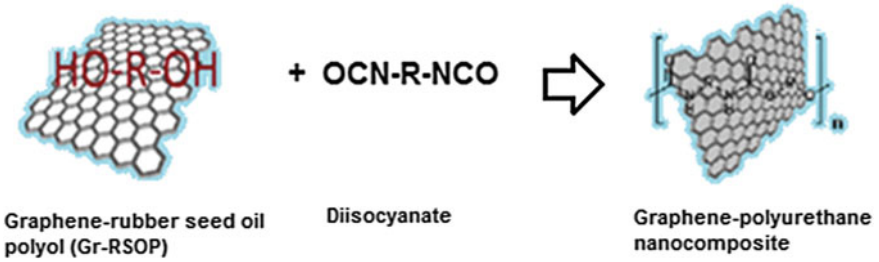

Fig. 2 Preparation of graphene-reinforced polyurethane nanocomposites

flasks, and the mixture was stirred and de-gassed, and then poured into a pre-greased mold to give graphene-reinforced polyurethane (Gr–PUH) and neat polyurethane (PUH) samples. The samples (Gr–PUH and PUH) were cured for about 2 h at 60 °C, and finally for about 12 h at 100 °C. This process was repeated using MDI as the polyisocyanate to give Gr–PUM and PUM samples. Figure 2 is a schematic representation of the reaction processes. The graphene loading per nanocomposites prepared was about 0.13%, based on the content of polyol.

Results and Discussion

Morphology of polyurethane nanocomposites

Insight into the degree of nanodispersion of the polyurethane nanocomposites was evaluated with WAXD. From the XRD diffraction patterns of the nanocomposite and neat polyurethanes (Fig. 3), the amorphous nature of the polyurethane nanocomposites (Gr–PUH and Gr–PUM) with little crystallinity, similar to the neat polyurethanes (PUH and PUM), is revealed. Thus, the molecules of the polyurethanes and nanocomposites are mainly irregularly packed with disordered orientation. This is due to the fact that polymers are composed of low atomic number elements with small atomic scattering factors and have only small content of crystal present [38]. For comparison, the XRD pattern of graphite (G), graphene oxide (GO), graphene nanosheet

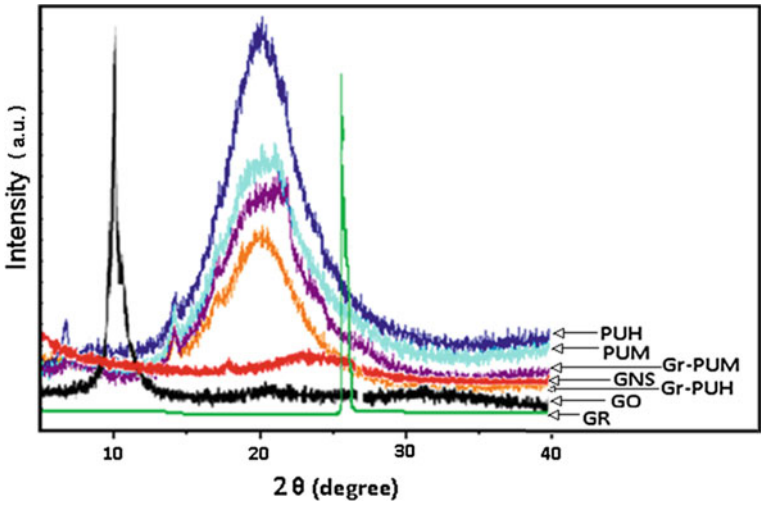

Fig. 3 X-ray diffractions of graphite, graphene nanosheets, graphene oxide, HMDI and MDI polyurethanes and their graphene-reinforced nanocomposites

(GNS), and Gr-PUs are shown with their characteristic peaks. The absence of the sharp planar (hexagonal arrangement of carbons) peak of graphite at about 27.4° in the 2θ degree of the Gr–PU XRD is an indication of the absence of graphite. Suffice to say also that it affirms to the fact that graphite was not oxidized to its oxide (GO) in the processing stage, nor did it remains in the graphite state. This could only point to the fact that there was successful dispersion (exfoliation) of graphite in ethanol/water mixture to single and few layered graphene nanosheets according to the technique reported by Liu et al. [15], neither did it restack or agglomerate back to graphite in the course of its dispersion into RSOP, nor in the preparation of the polyurethane nanocomposites. This is further confirmed by the XRD of the exfoliated graphene, which shows no prominent peak, except a very little hump (23–27°) subsumed in the halo peaks of the polyurethanes. And there are no other visible peaks in this region in the XRD of the nanocomposites that suggest otherwise.

The tapping mode AFM technique was also used in the morphological study of the samples. In Fig. 4a, b are shown the soft (dark) and hard (bright) domain segments of pristine polyurethanes elastomeric PUH and the rigid PUM surfaces, which are typical with polyurethanes. Detailed information on the nature and dimension of the dispersed phase on the continuous matrix phase, as seen in Fig. 4c, was not possible due to confusion with the characteristic segmentation domains of the polyurethanes and absence of SEM and TEM analysis of samples. However, the surface roughness as average Root Mean Square (Rq) values of Gr–PUH (10.13 nm) and Gr–PUM1 (21.8 nm) which are higher than those of the pristine polyurethanes (PUH and PUM), with an average Root Mean Square (Rq) values of 7.125 nm and

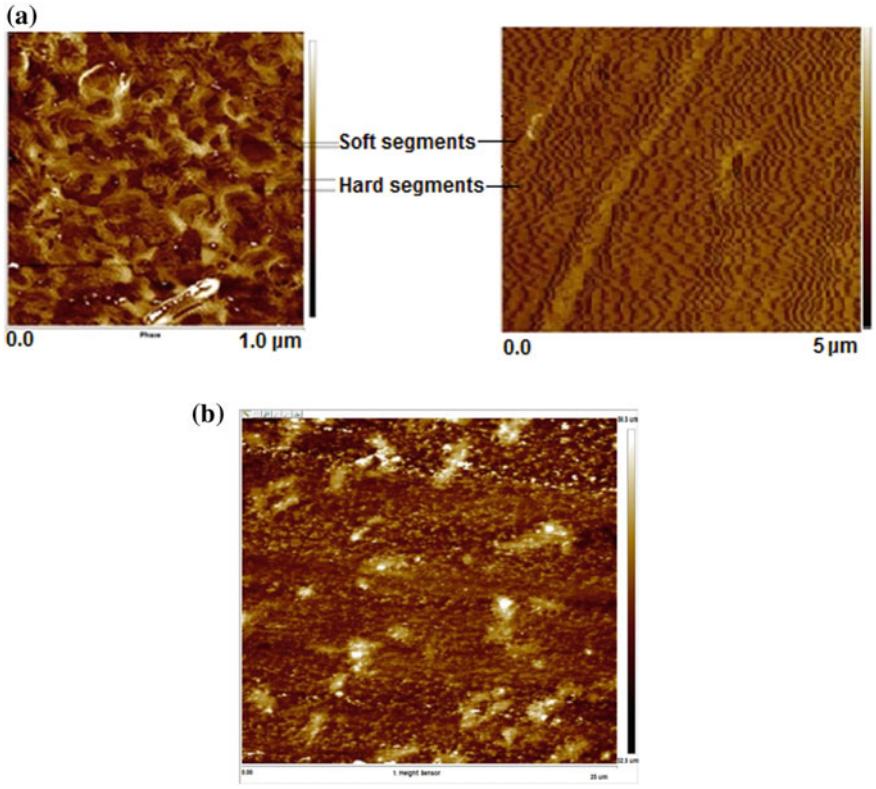

Fig. 4 **a** AFM of PUH and PUM showing the segment, **b** AFM of Gr–PUH

19.25 nm, respectively, was obtained with the AFM. This increase in surface roughness of the graphene-reinforced polyurethane nanocomposites could be attributed to the inclusion of the graphene nanosheet fillers.

The FTIR is a vital instrument used in the structural elucidation of polyurethane, as it gives very vital information of two major band regions, namely, the urethane linkage-NH region and the carbonyl (−C = O) region of the polymer. The FTIR spectra of the polyurethanes and their nanocomposites (Gr–PUH and Gr–PUM) are shown in Fig. 5a, b and are observed to be very similar with their respective pristine polymer. The spectra show the typical donor N-H and acceptor C = O stretching absorption bands of polyurethane at 3300–3360 cm^{-1} and 16950–1735 cm^{-1}, respectively, the asymmetric and symmetric stretching absorption bands of CH (2865–297) and present in the MDI derivatives are the C = C in-plane aromatic peaks. In the carbonyl region, the presence of the associated and non-associated stretching bands, which represents the level of H-bonding and free or non-hydrogen bonding within the

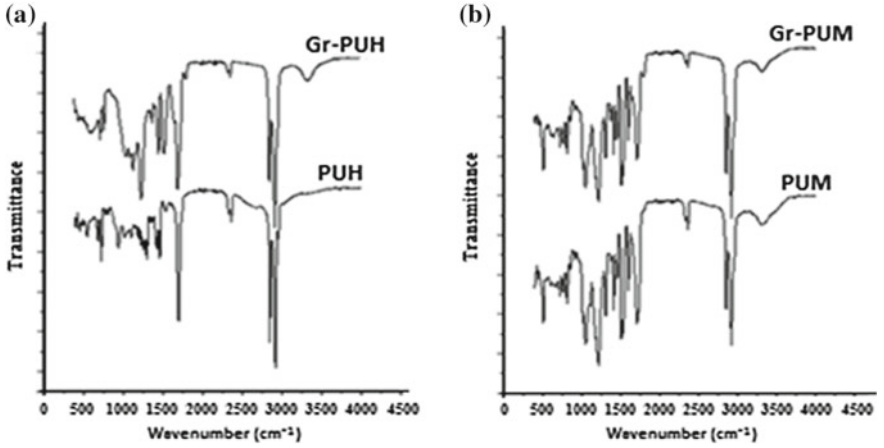

Fig. 5 FTIR of **a** HMDI polyurethane, PUH, and graphene polyurethane nanocomposite (Gr–PUH). **b** IR of MDI polyurethane (PUM) and graphene polyurethane nanocomposite (GrPUM)

urethanes structures, is visible. It is observed that the peaks of the H-bonded C = O are more intense and broad, which also reflects the level of inter-molecular activities in the network. There is an exceptional little shoulder around 1785–1800 cm^{-1}, present in the two nanocomposites spectra, absent in those of the pristine polyurethanes.

Mechanical Properties

Pristine graphene is reported to have the highest theoretical strength of all recorded known materials [44], and it is expected that this will greatly impart on physico-mechanical properties of the polyurethanes, such as hardness (ability to resist indentation), strength and modulus, thermal stability, etc., where there is proper mixing and exfoliation (Table 3).

Table 3 Physico-mechanical properties of polymer and nanocomposites

Sample	Young's modulus (GPa)	Average hardness (Mpa)	Tensile strength (Mpa)	Total elongation (MPa)	Ultimate true stress (MPa)	Yield stress (MPa)	Swelling @30° C (%)
PUH	0.016 ± 001	1.399 ± 001	2.09	187	5.93	2.09	1. 58
Gr–PUH	0.020 ± 002	1.580 ± 003	2.12	83.9	3.92	1.75	1.54
PUM	1.963 ± 001	60.50 ± 001	5.17	161	12.6	5.17	1.51
Gr–PUM	2.967 ± 001	136.92 ± 001	8.56	113	9.08	7.68	1.46

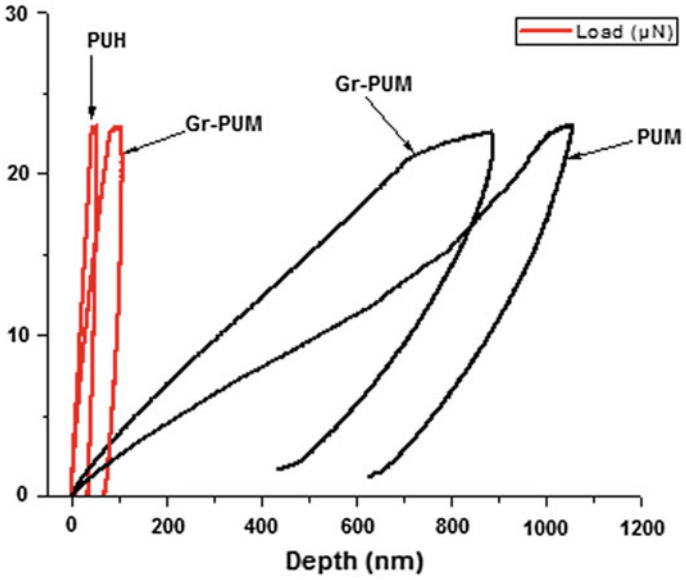

Fig. 6 Loading–unloading curves of polyurethanes and nanocomposites

Hardness

The loading–unloading curves of the polyurethanes (PUH and PUM), which are soft and rigid, respectively, and the nanocomposites (Gr–PUH and Gr–PUM), which are both rigid, are shown in Fig. 6 GR–PUH and Gr–PUM with about 12.9% and 126.2%, respectively, from the pristine PUH and PUM. The relatively high level of improvement recorded in Gr–PUM compared to Gr–PUH could be due to the combinative effect of graphene's hardness, brought to fore by good dispersion and interaction at the interphase, and the rigid nature of the pristine aromatic polyurethane facilitated by Van der Waals forces and hydrogen-bond interactions [44].

Tensile Strength and Modulus

The stress–strain curves of PH, PUM, Gr–PUH and Gr–PUM are shown in Fig. 7, and it is seen that there is an increase in the tensile strength of the nanocomposites relative to the unfilled polyurethanes, which led to 1.4 and 65.57% increase in Gr–PUH and Gr–PUM, respectively. The comparatively lesser improvement in Gr–PUH could be due to the inability of the graphene nanosheet and the polyurethane matrix

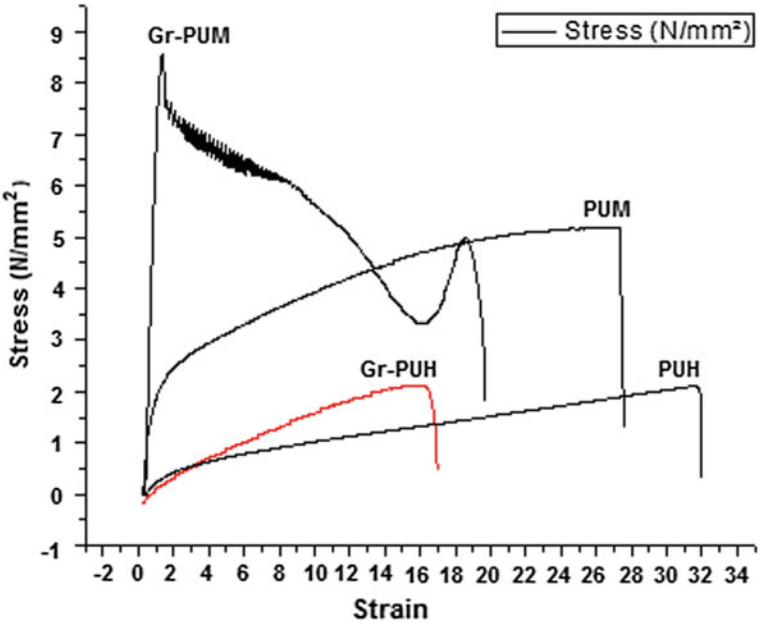

Fig. 7 Stress–strain curves of polyurethanes and nanocomposites

to have an optimized intereactivity at the interphases, resulting in the very low force of intimacy or homogeneity. This explanation is supported by the drastic reduction in its elongation at break, which is 83.9% (about 55.1% reduction from PUH), however. There was no sign of graphene stacking, as evidenced in the lack of the graphitic peak in the Gr–PUs X-ray diffractions. The relatively high increment in Gr–PUM could be due to relatively good dispersion and interaction at the interphases of the graphene sheets and polymer matrix, in addition to the rigid nature of the aromatic diisocyanate based polyurethane, resulting from higher H-bonding content, the effect of the aromatic ring, and higher crosslink in the network.

The Young's modulus is observed to increase by 25 and 51.1% in Gr–PUH and Gr–PUM. However, these increments in hardness and strength were followed by a corresponding decrease in elongation at break. As stated earlier, the unprecedented reduction in the elongation in Gr–PUH could be due to the failure at the interfacial region which did not have optimum interaction at the interphase of the graphene nanosheet and matrix of the polymer. Also, there is a reduction in the ultimate true stress in Gr–PUH and Gr–PUM, while yield stress increased in Gr–PUM and decreased in Gr–PUH. There is generally some improvement in the mechanical property of the polyurethane nancomposites (see Fig. 8), which could be ascribed to the impact of the presence of graphene reinforcement.

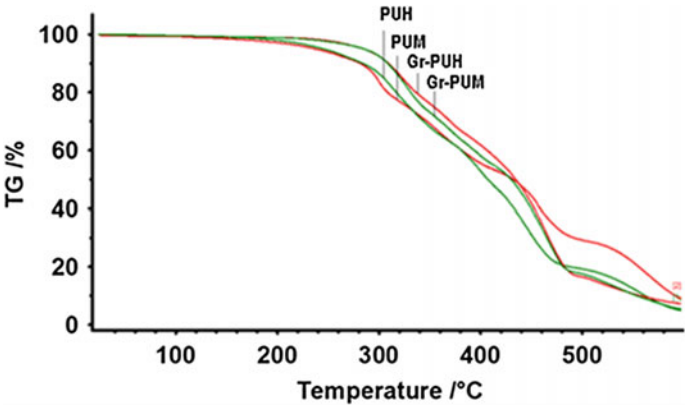

Fig. 8 Thermograms of polyurethanes and nanocomposites

Thermal Stability

The TGA results of the nanocomposites are listed in Table 4, while the respective thermograms are shown in Fig. 8.

The onset of degradation was at 250 °C for Gr–PUH and Gr–PUM each, representing an increment of about 23.7% and 219%, respectively, compared to the pristine polyurethanes. There is an increase in the temperature of the first step of degradation from 298°C to 297°C in PUH and PUM, to 310 °C, in Gr–PUH and Gr–PUM, i.e., about 4.0% and 4.1% increase, respectively. However, it was observed that unlike the pristine PUH, Gr–PUH thermogram had three steps, with the middle step not as pronounced, showing some level of stability at about 419 °C, which could be ascribed to the aromatic rings present in graphene.

This same step is seen in the thermograms of PUM and Gr–PUM, which is the middle or second degradation step, also due to degradation of the aromatic ring from the MDI aromatic ring, occurring at temperature of 430 °C.

Table 4 Thermal properties of Polyurethanes

Sample	Onset (°C)	First step (°C)	Second step (°C)	Third step (°C)
PUH1	202	298	515	–
Gr–PUH	255	310	420	530
PUM1	205	297	430	520
Gr–PUM	255	310	430	510

Conclusions

1. Graphene (mono- and few layered) sheets prepared by the method of Liu et al. [15], via aqueous liquid-phase technique, were successfully dispersed in RSOP co-monomer without re-aggregation, and used to prepare RSO polyol based graphene–polyurethane nanocomposites.
2. The inclusion of graphene brought about improvement in some of the properties of the nanocomposites.
3. It is quite impressive to note that at filler level of about 0.13% there is improvement in some properties of polyurethane nanocomposites.
4. This inclusion must satisfy certain conditions, such as good dispersion and/or optimized interactions at the interphases, for significant improvement to be obtained, as seen in Gr–PUH and Gr–PUM.

Acknowledgements The authors wish to acknowledge with gratitude Prof. Timothy Gonsalves, the Director of Indian Institute of Technology Mandi, Himachal Pradesh, India, for the Research Internship granted to EOO that made this possible, and Prof. I.O. Eguavoen, the Executive Director of Rubber Research Institute of Nigeria for the research leave granted to EOO.

References

1. Inagaki M, Tashiro R, Washino Y, Toyoda M (2004) J Phys Chem Solids 65:133
2. Chung DDL (1987) J Mater Sci 22:4190
3. Novoselov KS, Geim AK, Morozov SV, Jiang D, Zhang Y, Dubonos SV, Grigorieva IV, Firsov AA (2004) electric field effect in atomically thin carbon films. Science 306(5696):666–669
4. Nandamuri G, Roumimov S, Solanki R (2010) Chemical vapor deposition of graphene films. Nanotechnology 21–145604
5. Bae S, Kim H, Lee Y, Xu X, Park JS, Zheng Y, Balakrishnan J, Lei T, Ri KH, Song YI, Kim YJ, Kim KS, Ozyilmaz B, Ahn JH, Hong BH, Iijima S (2010) Roll-to-roll production of 30-inch graphene films for transparent electrodes. Nat Nano 5(8):574–578
6. Shivaraman S, Barton RA, Yu X, Alden J, Herman L, Chandrashekhar MVS, Park J, Mc Euen PL, Parpia JM, Craighead HG, Spencer MG (2009) Free-standing epitaxial graphene. Nano Lett 9(9):3100–3105
7. Aristov VY, Urbanik G, Kummer K, Vyalikh DV, Molodtsova OV, Preobrajenski AB, Zakharov AA, Hess C, Hänke T, Büchner B, Vobornik I, Fujii J, Panaccione G, Ossipyan YA, Knupfer M (2010) Graphene synthesis on cubic sic/si wafers. Perspectives for mass production of graphene-based electronic devices. Nano Lett 10(3):992–995
8. Emtsev KV, Bostwick A, Horn K, Jobst J, Kellogg GL, Ley L, Mc Chesney JL, Ohta T, Reshanov SA, Rohrl J, Rotenberg E, Schmid AK, Waldmann D, Weber HB, Seyller T (2009) Towards wafer-size graphene layers by atmospheric pressure graphitization of silicon carbide. Nat Mater 8(3):203–207
9. Deng D, Pan X, Zhang H, Fu Q, Tan D, Bao X (2010) Frees tanding graphene by thermal splitting of silicon carbide granules. Adv Mater 22(19):2168–2171
10. Cui X, Zhang C, Hao R, Hou Y (2011) Liquid-phase exfoliation, functionalization and application of graphene, nanoscale 3:2118–2126
11. Mittal V (2012) Polymer–Graphene nanocomposites. RSC nanoscience & nanotechnology No. 26. The Royal Society of Chemistry. Published by the Royal Society of Chemistry, www.rsc.org

12. Allen ML, Tung VC, Kaner RB (2010) honeycomb carbon: a review of graphene. Chem Rev 2010(110):132–145
13. Chen Z, Chisholm B, Patani R, Wu J, Fernando S, Jogodzinski K, Webster D (2010) Soybased UV-curable thiol–ene coatings. J Coat Technol Res 7:603–613
14. Xu M, Zhang W, Yang Z, Yu F, Ma Y, Hu N, He D, Liang Q, Su Y, Zhang Y (2015) One-pot liquid-phase exfoliation from graphite to graphene with carbon quantum dots. Nanoscale 7:10527–10534
15. Liu W, Bao-Yu Xia B-Y, Xiao-Xia Wang X-X, Wang J-N (2012) Exfoliation and dispersion of graphene in ethanol-water mixtures. Front Mater Sci 6(2):176–182
16. Meyer JC, Geim AK, Katsnelson MI, Novoselov KS, Booth TJ, Roth S (2007) Nature 446:60
17. Lee C, Wei X, Kysar JW, Hone J (2008) Science 321:385
18. Sham AYW, Notley SM (2013) A review of fundamental properties and applications of polymer–graphene hybrid materials. Soft Matter 9:6645–6653
19. Zhang YB, Small JP, Amori MES, Kim P (2005) Phys Rev Lett 94:176–803
20. Su CY, Xu YP, Zhang WJ et al (2009) Electrical and spectroscopic characterizations of ultra-large reduced graphene oxide monolayers. Chem Mater 21(23):5674–5680
21. Stoller MD, Park S, Zhu Y et al (2008) Graphene-based ultracapacitors. Nano Lett 8(10):3498–3502
22. Lin YM, Jenkins KA, Valdes-Garcia A et al (2009) Operation of graphene transistors at gigahertz frequencies. Nano Lett 9(1):422–426
23. Si YC, Samulski ET (2008) Exfoliated graphene separated by platinum nanoparticles. Chem Mater 20(21):679–6792
24. Skaltsas T, Karousis N, Yan H-J, Wang C-R, Pispas S, Tagmatarchis N (2012) Graphene exfoliation in organic solvents and switching solubility in aqueous media with the aid of amphiphilic bock copolymers. J Mater Chem 2012(22):21507
25. Gómez-Navarro C, Weitz RT, Bittner AM et al (2007) Electronic transport properties of individual chemically reduced graphene oxide sheets. Nano Lett 7(11):3499–3503
26. Dimiev A, Kosynkin DV, Alemany LB et al (2012) Pristine graphite oxide. J Am Chem Soc 134(5):2815–2822
27. Tung VC, Allen MJ, Yang Y et al (2009) High-throughput solution processing of large-scale graphene. Nat Nanotechnol 4(1):25–29
28. Stankovich S, Dikin DA, Dommett GHB, Kohlhaas KM, Zimney EJ, Stach EA, Piner RD, Nguyen ST, Ruoff RS (2006) Nature 442(7100):282–286
29. Luo Z, Lu Y, Somers LA et al (2009) High yield preparation of macroscopic graphene oxide membranes. J Am Chem Soc 131(3):898–899
30. Tang LH, Wang Y, Li YM et al (2009) Preparation, structure, and electrochemical properties of reduced graphene sheet films. Adv Func Mater 19(17):2782–2789
31. Notley SM (2012) Langmuir 28:14110–14113
32. Zheng W, Wong S-C (2003) Compos. Sci. Technol. 63(2):225–235
33. Zheng W, Wong S-C, Sue H-J (2002) Polymer 73(25):6767–6773
34. Xu J, Hu Y, Song L, Wang Q, Fan W, Liao G, Chen Z (2001) Polym Degrad Stab 73(1):29–31
35. Sadasivuni KK, Ponnamma D, Kim J, Thomas S (eds) (2015) Graphene-based polymer nanocomposite in electronics, VI, 382 p 175. ISBN 978-3-319-13874-9
36. Jing-Wei S, Xiao-Mei C, Wen-Yi H (2003) J Appl Polym Sci 88(7):1864–1869
37. Liu PG, Xiao P, Xiao M, Gong K-C (2000) Chin J Polym Sci 18(5):413–418. Wenge Z, Xuehong L, Shing-Chung WJ (2004) Appl Polym Sci, 91(5):2781–2788
38. Kim H, Abdala AA, Macosko CW (2010) Graphen/polymer nanocomposites. Macromolecules 43:6515–6530
39. Kuilla T, Bhadra S, Yao D, Kim NH, Bose S, Lee JH (2010) Recent advances in graphene based polymer composites. Prog Mater Sci 35:1350–1375
40. Yang D, Velamakanni A, Bozoklu G et al (2009) Chemical analysis of graphene oxide films after heat and chemical treatments by X-ray photoelectron and Micro-Raman spectroscopy. Carbon 47(1):145–152

41. Liu S, Tian M, Yan B, Yao Y, Zhang L, Nishi T (2015) High performance dielectric elastomers by partially reduced graphene oxide and disruption of hydrogen bonding of polyurethanes. Polymer 56:375–384
42. Obazee EO (2018) PhD Thesis. Biobased polymers from modified rubber seed oil, University of Benin City, Benin City
43. Ferrer CC, Babb D, Ryan AJ (2008) Characterization of polyurethane networks based on vegetable derived polyol. Polymer 49:3279–3287
44. Singh V, Joung D, Zhai L, Das S, Khondaker SI, Seal S (2011) Graphene based materials: past, present and future. Prog Mater Sci 56:1178–1271